

## An Approach Towards the Fabrication of Flexible Piezoelectric Composite Film of Ca-Doped ZnO/PVDF for Energy Harvesting Application

Garima<sup>1</sup>, and Bhukkal, Suman<sup>2</sup>

<sup>1&2</sup>Department of Applied Chemistry, NIILM University, Kaithal Haryana

Orchid Id: 0009-0008-6594-1924

DOI: <https://doi.org/10.70388/ijabs250104>

Received on Sep 20, 2024

Accepted on Nov 20, 2024

Published on Jan 01, 2025

This article is licensed under a license [Commons Attribution-NonCommercial-NoDerivatives 4.0 International Public License \(CC BY-NC-ND 4.0\)](#)

### Abstract

In the present time, there is a gradual increase in the demand for energy, especially green energy; therefore, significant advancements have occurred in the field of energy harvesting in recent years to meet the growing demand for portable, sustainable, and renewable energy sources. Corresponding gadgets are specifically engineered to capture and transform the surrounding energies into practical electrical energy. Using piezoelectric material, we are working to increase the energy output voltage from this material using different techniques. In this reported work, we synthesize the ZnO and Ca-doped ZnO (CaZ) powder with the help of the co-precipitation method calcined at 650° C. X-ray diffraction (XRD) confirmed the prepared ceramic powders' phase formation. The calcined ZnO and Ca-doped ZnO (CaZ) particles were mixed with PVDF to prepare flexible composite films of 5 wt. % with a thickness of ~60 μm by drop cast method. Structural analysis of the fabricated flexible composite film was performed by XRD and Fourier Transform Infrared (FTIR) spectroscopy, which indicated the formation of the β-β-phase in the composite film. SEM images were used to analyze the composite film's morphology and structure. The fabricated devices' energy harvesting performance was measured with a shaker's help. Then, a voltage output is measured by making electrical connections with the flexible films. The voltage output is 3.76V, 18.9V, and 21.8 V, respectively, for PVDF, 5 wt. % of ZnO and CaZ fillers with PVDF can run various small electrical devices.

**Keywords:** Piezoelectric, PVDF, Composite films, Microstructure

Garima, & Bhukkal, S.

28

## Introduction

As humans develop in the global society, we need more and more energy to fulfill our requirements. The current energy problem, caused by a scarcity of fossil fuels, has prompted the Explore several renewable energy sources, including hydroelectric, wind, solar, and others. Mechanical vibration is an attractive source of ambient energy due to its convenient accessibility and compatibility with piezoelectric materials; it has the potential to convert mechanical stress energy into electrical energy. Following that, various efforts have been made to create ways to convert mechanical to electrical energy [1-5]. Several inorganic piezoelectric materials, including barium titanate (BaTiO<sub>3</sub>), zinc oxide (ZnO), and lead zirconia titanate (PZT) and others, have been extensively used in energy scavenging applications [6-10]. The first documented nanogenerator was an array of ZnO nanowires [11]. Later, other nanogenerators employing various additional piezo materials were reported to power small-size electronic devices. Having piezoelectric properties, polymers, such as poly(vinylidene fluoride) (PVDF) and its derivatives, are well-suited for overcoming the drawbacks of ceramic-based piezoelectric materials, particularly their susceptibility to breakage. These polymers are eco-friendly, compatible with living organisms, and easy to produce. The fluorine and hydrogen atoms in PVDF's repeating unit (-CH<sub>2</sub>-CF<sub>2</sub>-) form several polar and non-polar configurations, including  $\alpha$ ,  $\beta$ ,  $\gamma$ , and  $\delta$  phases [12]. Polar in nature,  $\beta$ -phase PVDF with all-trans conformation (TTTT) has superior piezoelectric characteristics, making it ideal for energy harvesting applications [13-16]. Furthermore, the copolymerization approach has resulted in several PVDF copolymers with comparable piezoelectric characteristics. The substitution of a hydrogen atom with an additional fluorine atom results in steric hindrance and modifies the potential energy of the polymer chains, rendering it appropriate for exclusively trans conformation [17-18]. However, as we compared them to ceramic properties, polymers have lesser piezoelectric capabilities, demanding the introduction of specific piezoelectric particles. The significant piezoelectric coupling factor of ZnO nanostructure makes it a highly researched semiconducting material. Furthermore, their lack of toxicity and ability to interact well with living organisms make them extremely valuable in the majority of energy-harvesting systems. The simplicity of changing and adding external features further broadens their uses. Various attempts have been made to improve the piezoelectric efficiency of nanogenerators manufactured from diverse piezoelectric polymer composites [19-25].

Research has demonstrated that utilizing non-ferroelectric ZnO in conjunction with piezoelectric polymers enhances the performance of piezoelectric devices. This combination

produces a flexible nanogenerator with a larger electrical output [26-30]. Research has focused on increasing polymer or filler qualities by chain modifications or dopant ion addition to nanofiller to enhance performance. Various piezoelectric nanofillers have been mixed with PVDF copolymers and terpolymers, while dopant ions and molecules have been used to modify ZnO nanostructures. These modifications aim to enhance the performance of piezoelectric devices [31-34].

A unique piezoelectric energy harvesting device was created using a straightforward technique, mixing PVDF polymer with calcium ion-doped ZnO(CaZ) nanoparticles that had not been described before. Ca-doped ZnO particles synthesized using the co-precipitation technique were used as a ceramic filler in the polymer matrix. Several crystallographic and morphological investigations were conducted to confirm the integration of calcium (Ca) into the crystalline structure of zinc oxide (ZnO) in the generated nanofiller. The CaZ/PVDF composite film was deposited by drop casting a solution and used as a thin active layer in a piezoelectric energy harvesting device.

Prior to manufacturing the ultimate device, an examination was conducted on the crystalline and morphological properties of the synthesized films. The piezoelectric performance of the films was evaluated in comparison to a pure PVDF film, and the underlying mechanism responsible for the enhanced performance of the films was also investigated. Ultimately, the sensing capability of the fabricated devices was assessed in the presence of fluctuating pressures.

## 2. Materials and Methodology

### 2.1 Synthesis of CaZ filler:

Zinc chloride and calcium chloride are utilized as precursors to synthesize stoichiometric  $Zn_{(1-x)}Ca_{(x)}O$  ( $x = 0.05$ ) nanoparticles using the co-precipitation approach, which has been previously employed in similar studies [35]. Zinc chloride and calcium chloride dissolved separately in de-ionized water at room temperature on a magnetic stirrer. The two solutions were then combined to form a homogeneous solution. After 1 hour of continuous stirring, a 0.1 M NaOH (Sodium Hydroxide) solution was added slowly to the zinc and calcium chloride mixture. The precipitates were collected via centrifugation and then washed repeatedly with de-ionized water and ethanol to remove any residual chemicals. The precipitate was dehydrated

in a hot air oven at a temperature of 70°C for an extended period of time and subsequently subjected to calcination at a temperature of 600°C for a duration of 2 hours in a furnace, resulting in the formation of Ca-doped ZnO particles. Zinc oxide particles were made using the same technique described above, excluding adding the calcium precursor calcium chloride.

## **2.2 Synthesis of Ca-doped ZnO/PVDF composite film**

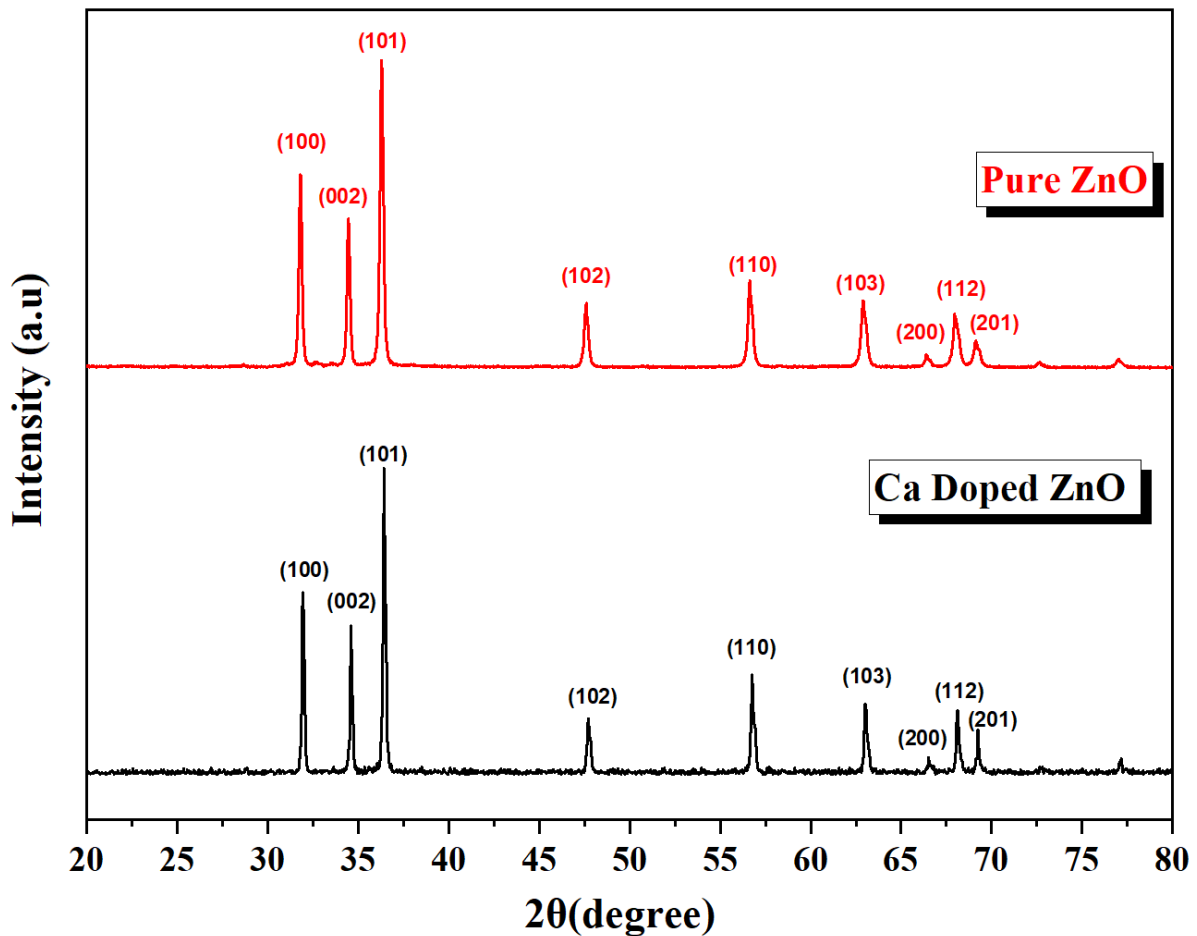
A precise amount of PVDF was dissolved in N’N’-dimethylformamide (DMF) and agitated using a magnetic stirrer at a temperature of 45 degrees Celsius for a duration of 2 hours in order to obtain a homogeneous and transparent solution. Subsequently, particles of  $Zn_{(1-0.05)}Ca_{0.05}O$  were incorporated into the solution created earlier, with a concentration of 5wt. % relative to the polymer matrix. The mixture was then agitated for an additional 3 hours. Next, the evenly distributed solution was applied onto a pristine glass petri dish to create a composite film of Ca-doped ZnO/PVDF. The film was dried in a hot air oven at 80°C until the solvent had evaporated.

## **3. Material Characterisation**

The crystal structure of the  $Zn_{(1-0.05)}Ca_{0.05}O$  particles and composite films were analysed using an X-ray diffractometer (PAN analytical X’pert PRO). The experiment involved exposing the sample to radiation with a wavelength of 1.5406 Å, over a range of 2θ angles from 120° to 80° for powder and 10° to 80° for composite films. The morphology of the CaZ/PVDF composite films was analysed using scanning electron microscopy (SEM) with a Zeiss EVO40 apparatus from JNU, India. The effect of CaZ particles on composite film's phase crystallization was further studied using a Fourier transform infrared spectrometer (FTIR, Thermo Scientific).

## **4. Results and Discussion.**

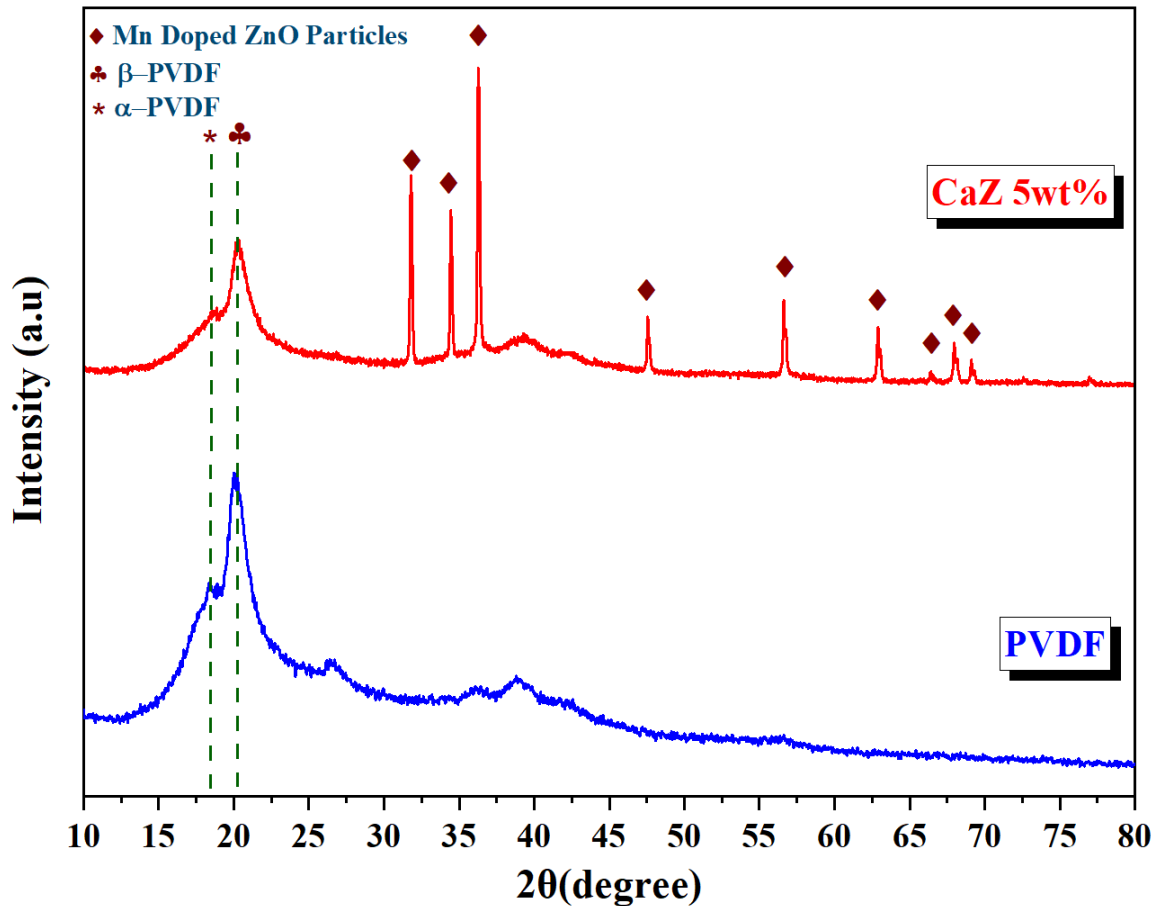
4.1 Analysing the structure and microscopic properties of CaZ ceramic powder.



**Fig. 1.** XRD Analysis of ZnO and CaZ ceramic powder

Fig. 1 shows the powder X-ray diffraction patterns for both unmodified ZnO and Ca-doped ZnO (CaZ) particles. ZnO, a wideband semiconducting inorganic material, can exist in two primary crystalline forms: zinc wurtzite and zinc blende. The Wurtzite structure of ZnO, characterized by its two polar surfaces of Zn and O, generates a dipole moment and spontaneous polarization along the c-axis, which endows ZnO with piezoelectric properties [36]. These peaks align closely with the pure ZnO crystalline structure as referenced in the JCPDS database (card number: 361451), confirming the hexagonal wurtzite phase of ZnO [37]. The inclusion of calcium as a dopant does not significantly alter the diffraction pattern of the ZnO crystal structure. The absence of additional peaks suggests that Ca ions substitute Zn ions in the lattice points without disrupting the hexagonal wurtzite structure. However, the diffraction peak intensity for CaZ nanoparticles is lower than unmodified ZnO, indicating the successful substitution of Zn ions with Ca dopant ions [38].

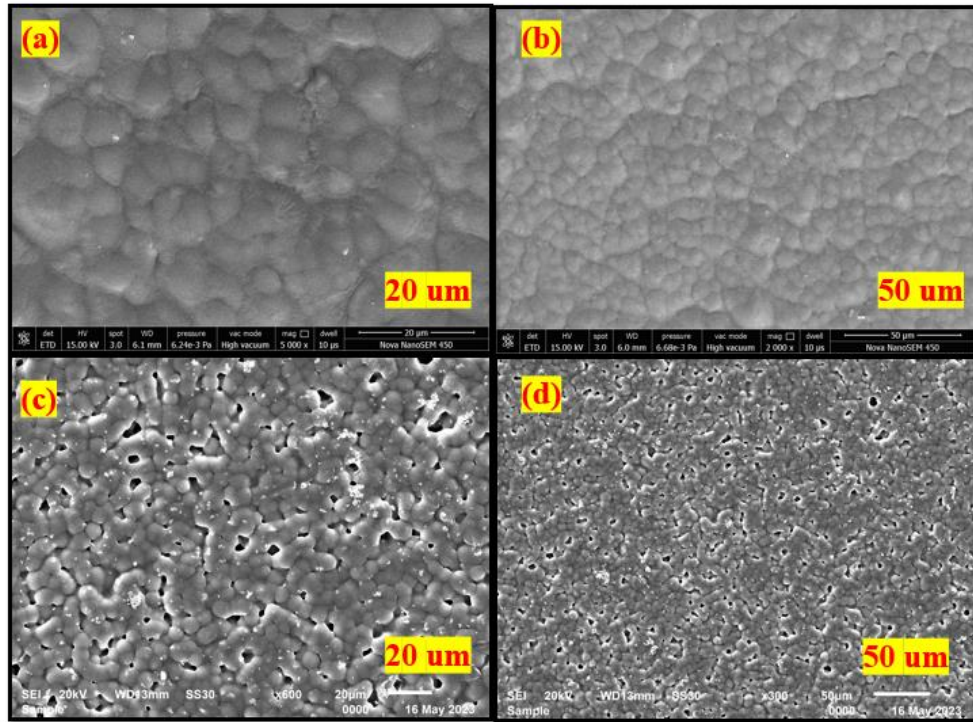
#### 4.2 Analysis of the structure of a composite film of PVDF and CaZ/PVDF



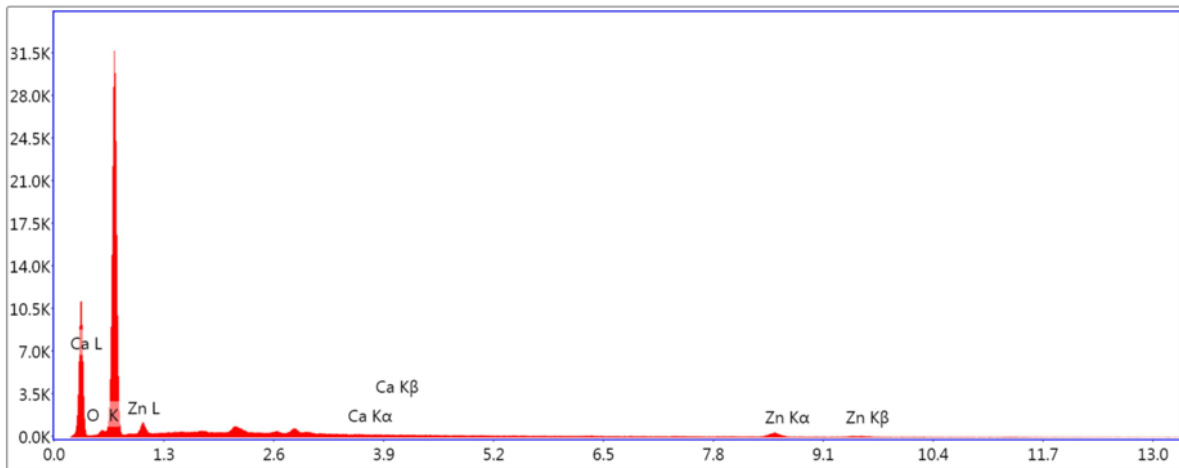
**Fig. 2.** The X-ray diffraction pattern of both pure PVDF and CaZ/PVDF composite film.

Fig. 2 displays the X-ray diffraction (XRD) patterns for pure PVDF film and a CaZ/PVDF composite film. In the pure PVDF film, both crystalline and amorphous diffraction peaks can be observed, highlighting its polycrystalline nature. A notable diffraction peak at  $20.4^\circ$  is attributed to the (110/200) planes of the electroactive polar  $\beta$  phase of PVDF. Additionally, a broad peak at  $18.0^\circ$  indicates the presence of the non-polar  $\alpha$ -phase, specifically reflecting the (020) plane. Peaks at  $35^\circ$  and  $41^\circ$  correspond to the polar  $\beta$ -phase, representing the (001) and (201) planes, respectively [39]. In the composite film, the increased intensity at the  $20.0^\circ$  peak and the decreased intensity at the  $18.0^\circ$  peak suggest a higher content of the polar  $\beta$ -phase. The comparison of the  $35^\circ$  peak between the composite and pure films indicates that the composite film's diffraction pattern combines the polymer and the filler. The significant peaks between  $30^\circ$  and  $36^\circ$  in the CaZ nanofillers suggest that the pattern in this region of the composite film indicates the presence of CaZ within the polymer matrix. The presence of both the  $\beta$ -phase polymer peak and the CaZ filler peak after incorporating CaZ into the PVDF polymer suggests that the CaZ fillers minimally affect the polymer chain's crystallographic alignment [40].

### 4.3. Morphological characterization of CaZ/PVDF composite films



**Fig. 3.** Sem images at 20 μm and 50μm of Pure PVDF 3(a) and 3(b), 5 wt.% CaZ/PVDF 3(c) and 3(d)



**Fig. 4.** EDS spectrum of the CaZ/PVDF composite film

Fig. 3 shows SEM images of the top surfaces of pure PVDF and CaZ/PVDF composite films. The pure PVDF film exhibits a smooth and flat surface, whereas the CaZ/PVDF composite film has a distinct surface texture. The air/solution interface of the composite film displays numerous spherical features, likely due to the presence of CaZ fillers [41]. The white regions

in the SEM image of the composite film indicate gaps between these spherical areas, while the small dot-like structures are the evenly distributed CaZ nanofillers on the polymer matrix surface [42]. Fig. 4 presents the Energy-dispersive X-ray spectroscopy (EDS) spectra for the composite film with 5 wt. % CaZ, showing peaks corresponding to Ca and ZnO, confirming their presence within the PVDF film.

#### 4.4 Fourier transform-infrared (FTIR) spectroscopy studies.

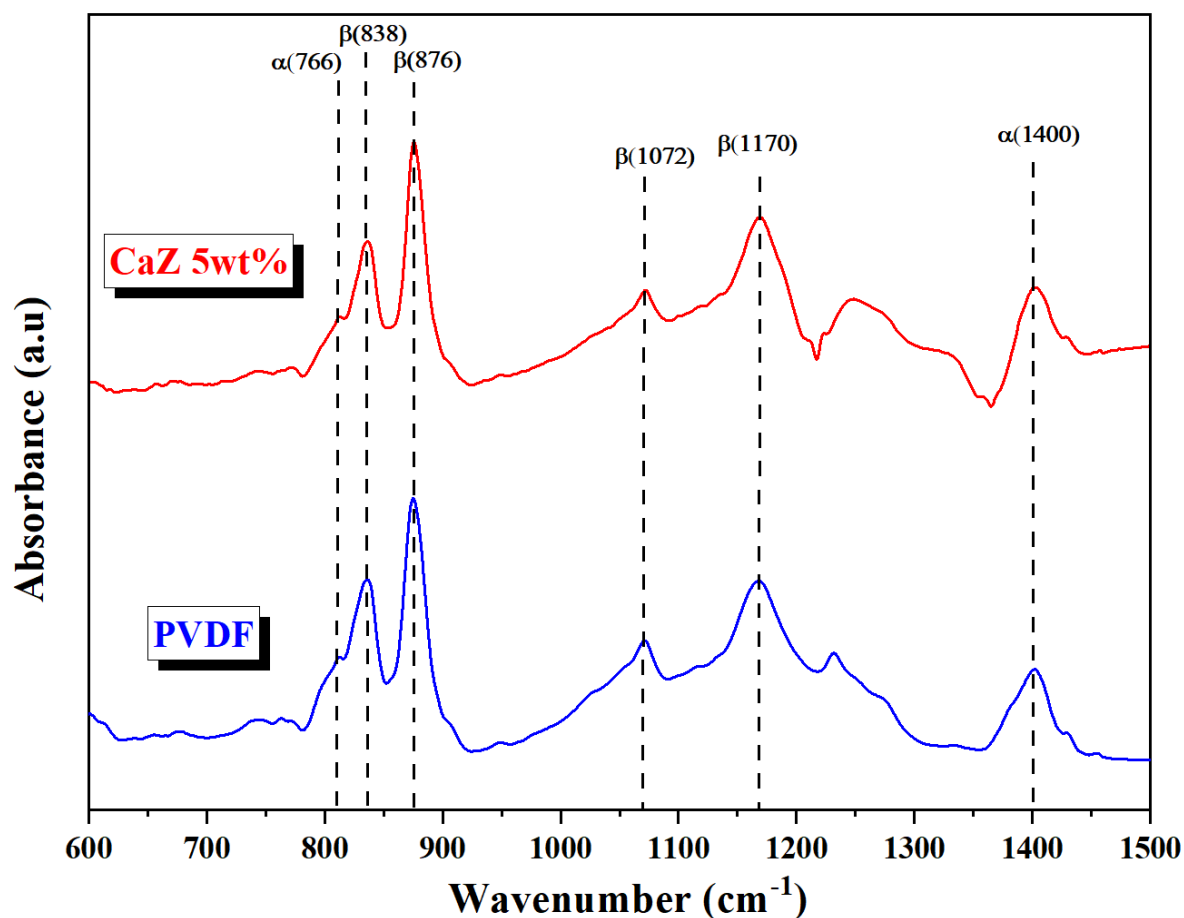


**Fig. 5** Shows the FTIR spectra of pure PVDF film and a composite film of 5 wt.% CaZ ceramics in the PVDF matrix.

FTIR research was conducted on both the pure and produced composite films to examine the impact of CaZ ceramic particles on the crystal structure of PVDF. The Fourier Transform Infrared (FTIR) spectra of a pure Polyvinylidene fluoride (PVDF) film and composite films made of CaZ and PVDF were obtained at ambient temperature. The spectra were recorded in the region of 600–1500  $\text{cm}^{-1}$  and are shown in Fig. 5. The FTIR spectra indicate the presence of both  $\alpha$  and  $\beta$  phases in all produced films. The peaks corresponding to the  $\alpha$  and  $\beta$  phases are indicated in Fig 5. The FTIR data obtained was consistent with the XRD data, indicating

the presence of the  $\beta$  phase of PVDF in both the pure PVDF films and the CaZ/PVDF composite films. The absorption bands seen at 766 and 1400  $\text{cm}^{-1}$  are identified as the distinctive peaks of the  $\alpha$  phase of PVDF [43-46]. Conversely, the absorption bands observed at 838, 876, 1072 and 1170  $\text{cm}^{-1}$  are identified as the distinctive peaks of the  $\beta$  phase of PVDF [47]. In addition, compared to the pure PVDF film, the absorption peaks corresponding to the  $\beta$  phase of PVDF were strengthened in all the CaZ/PVDF composite films. This suggests that the incorporation of CaZ ceramic powder in PVDF resulted in an improved crystallization of the  $\beta$  phase of PVDF. The  $\beta$  phase of PVDF plays a crucial role in enhancing the piezoelectric performance of the generator.

### 5. Piezoelectric properties of fabricated PEG devices.

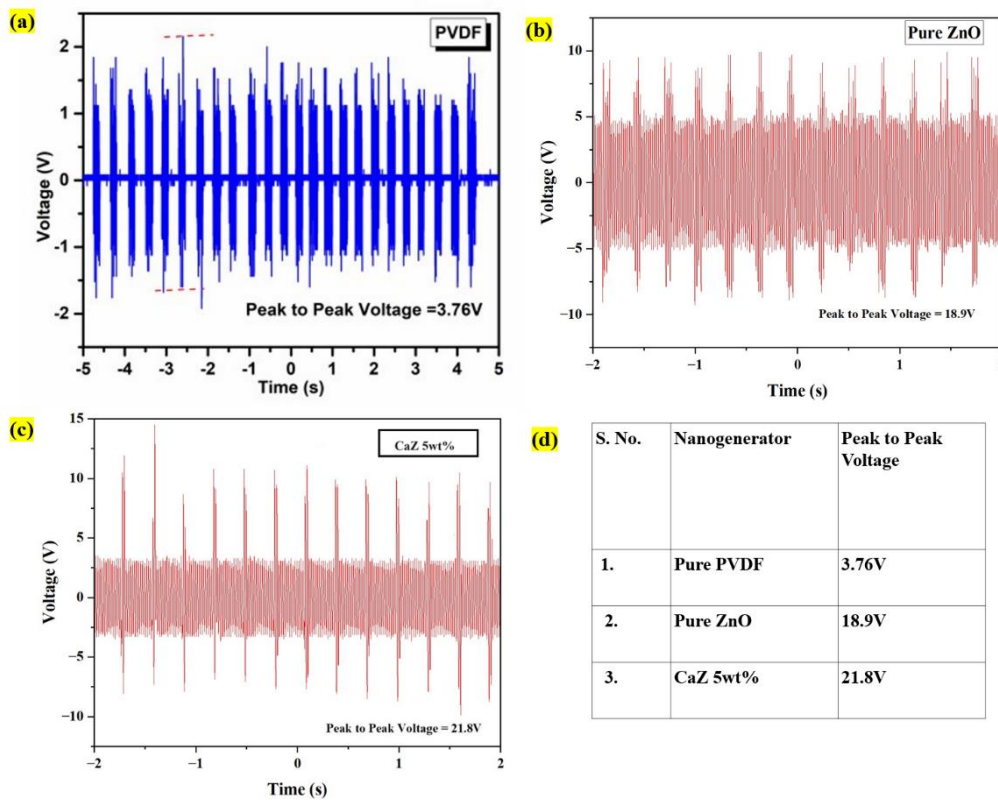


**Fig. 6.** Voltage output of the (a) PVDF (b) ZnO/PVDF (c) 5 wt.% CaZ.

Fig. 6(a), (b), and (c) display the voltage responses of three different devices were evaluated: one made of pure PVDF, a second incorporating ZnO/PVDF, and a third consisting of a CaZ/PVDF composite film. Testing was conducted without using a rectifier. The inclusion of CaZ fillers in the composite film significantly increased the voltage potential compared to both the pure PVDF and ZnO/PVDF devices. As shown in Fig. 6(d) and summarized in a table, the peak voltages of the composite film devices are highlighted over a short time span. The

generated voltage reached a maximum of 21.8 V for the CaZ/PVDF, 18.9 V for the ZnO/PVDF and 3.76 V for pure PVDF PEG. This voltage generation is due to the film's crystal structure deformation under applied stress, leading to the alignment of electric dipoles.

## 6. Conclusion

We successfully synthesized CaZ powder and analysed it using XRD techniques. Additionally, composite films created through the solvent casting technique were examined with XRD and FTIR to investigate their crystalline properties. The results show that incorporating CaZ enhances the polar electroactive phase, leading to increased crystallinity in the fillers. The CaZ content within the PVDF matrix affects various device characteristics and improves piezoelectric performance. The voltage output of the PEG was measured by applying force to the film using a shaker, and the CaZ/PVDF PEG achieved a maximum voltage output of 21.8 V

## References:

1. Abzan, N., Kharaziha, M., & Labbaf, S. (2019). Development of three-dimensional piezoelectric polyvinylidene fluoride-graphene oxide scaffold by non-solvent induced phase separation method for nerve tissue engineering. *Materials and Design*, 167, Article 107636. <https://doi.org/10.1016/j.matdes.2019.107636>
2. Badatya, S., Bharti, D. K., Srivastava, A. K., & Gupta, M. K. (2021). Solution processed high performance piezoelectric eggshell membrane– PVDF layer composite nanogenerator via tuning the interfacial polarization. *Journal of Alloys and Compounds*, 863, Article 158406 May. <https://doi.org/10.1016/j.jallcom.2020.158406>
3. Bae, S.-H., Kahya, O., Sharma, B. K., Kwon, J., Cho, H. J., Özyilmaz, B., & Ahn, J.-H. (2013). Graphene-P (VDF-TrFE) multilayer film for flexible applications. *ACS Nano*, 7(4), 3130–3138. <https://doi.org/10.1021/nn400848j>
4. Bhavanasi, V., Kumar, V., Parida, K., Wang, J., & Lee, P. S. (2016). Enhanced piezoelectric energy harvesting performance of flexible PVDF-TrFE bilayer films with graphene oxide. *ACS Applied Materials and Interfaces*, 8(1), 521–529. <https://doi.org/10.1021/acsami.5b09502>
5. Chen, J., Xiong, X., Zhang, Q., Shui, L., Shen, S., Yang, H., Zhu, Z., & Zhang, F. (2019). P(VDF-TrFE)/PMMA Blended Films with Enhanced Electrowetting

- Responses and Superior Energy Storage Performance. *Polymers*, 11(3), 526. <https://doi.org/10.3390/polym11030526>
6. Chen, S., Yao, K., Tay, F. E. H., & Chew, L. L. S. (2010). Comparative investigation of the structure and properties of ferroelectric poly (vinylidene fluoride) and poly (vinylidene fluoride–tri fluoroethylene) thin films crystallized on substrates. *Journal of Applied Polymer Science*, 116(6), 3331–3337. <https://doi.org/10.1002/app.31794>
  7. Chowdhury, A. R., Abdullah, A. M., Hussain, I., Lopez, J., Cantu, D., Gupta, S. K., Mao, Y., Danti, S., & Uddin, M. J. (2019). Lithium doped zinc oxide based flexible piezoelectric-triboelectric hybrid nanogenerator. *Nano Energy*, 61, 327–336. <https://doi.org/10.1016/j.nanoen.2019.04.085>
  8. Fakhri, P., Amini, B., Bagherzadeh, R., Kashfi, M., Latifi, M., Yavari, N., Asadi Kani, S. A., & Kong, L. (2019). Flexible hybrid structure piezoelectric nanogenerator based on ZnO nanorod/PVDF nanofibers with improved output. *RSC Advances*, 9(18), 10117–10123. <https://doi.org/10.1039/c8ra10315a>
  9. Garain, S., Jana, S., Sinha, T. K., & Mandal, D. (2016). Design of in situ poled Ce<sup>3+</sup>-doped electrospun PVDF/graphene composite nanofibers for fabrication of nano pressure sensor and ultrasensitive acoustic nanogenerator. *ACS Applied Materials and Interfaces*, 8(7), 4532–4540. <https://doi.org/10.1021/acsami.5b11356>
  10. Guo, D., Cai, K., Deng, P., Si, G., Sun, L., Chen, F., Ning, H., Jin, L., & Ma, J. (2020). Structure tailorable triple-phase and pure double-polar-phase flexible IF-WS<sub>2</sub>@ poly (vinylidene fluoride) nanocomposites with enhanced electrical and mechanical properties. *Journal of Materiomics*, 6(3), 563–572. <https://doi.org/10.1016/j.jmat.2020.04.004>
  11. Habibur, R. M., Yaqoob, U., Muhammad, S., Uddin, A. S. M. I., & Kim, H. C. (2018). the effect of RGO on dielectric and energy harvesting properties of P (VDF-TrFE) matrix by optimizing electroactive  $\beta$  phase without traditional polling process. *Materials Chemistry and Physics*, 215, 46–55. <https://doi.org/10.1016/j.matchemphys.2018.05.010>
  12. [39] R.M. Habibur, U. Yaqoob, S. Muhammad, A.I. Uddin and H.C. Kim, The effect of RGO on dielectric and energy harvesting properties of (PVDF-TrFE) matrix by optimizing electroactive  $\beta$  phase without traditional polling process, *Materials Chemistry and Physics*, 215 (2018) 46-55.

13. Hussain, M., Khan, A., Nur, O., Willander, M., & Broitman, E. (2014). The effect of oxygen plasma treatment on the mechanical and piezoelectrical properties of ZnO nanorods. *Chemical Physics Letters*, 608, 235–238. <https://doi.org/10.1016/j.cplett.2014.06.018>
14. Jeyachitra, R., Senthilnathan, V., & Senthil, T. S. (2018). Studies on electrical behaviour of Fe doped ZnO nanoparticles prepared via co-precipitation approach for photocatalytic application. *Journal of Materials Science: Materials in Electronics*, 29(2), 1189–1197. <https://doi.org/10.1007/s10854-017-8021-0>
15. Jin, L., Ma, S., Deng, W., Yan, C., Yang, T., Chu, X., Tian, G., Xiong, D., Lu, J., & Yang, W. (2018). Polarization-free high-crystallization  $\beta$ -PVDF piezoelectric nanogenerator toward self-powered 3D acceleration sensor. *Nano Energy*, 50, 632–638. <https://doi.org/10.1016/j.nanoen.2018.05.068>
16. Jing, Q., & Kar-Narayan, S. (2018). Nanostructured polymer-based piezoelectric and triboelectric materials and devices for energy harvesting applications. *Journal of Physics. Part D*, 51(30), Article 303001. <https://doi.org/10.1088/1361-6463/aac827>
17. Kaur, S., & Singh, D. P. (2020). On the structural, dielectric and energy storage behaviour of PVDF-CaCu<sub>3</sub>Ti<sub>4</sub>O<sub>12</sub> nanocomposite films. *Materials Chemistry and Physics*, 239, Article 122301. <https://doi.org/10.1016/j.matchemphys.2019.122301>
18. Koka, A., Zhou, Z., & Sodano, H. A. (2014). vertically aligned BaTiO<sub>3</sub> nanowire arrays for energy harvesting. *Energy Environ. Sci*, 7(1), 288–296. <https://doi.org/10.1039/C3EE42540A>
19. Lee, J. W., Cho, H. J., Chun, J., Kim, K. N., Kim, S., Ahn, C. W., Kim, I. W., Kim, J.-Y., Kim, S.-W., Yang, C., & Baik, J. M. (2017). Robust nanogenerators based on graft copolymers via control of dielectrics for remarkable output power enhancement. *Science Advances*, 3(5), Article e1602902. <https://doi.org/10.1126/sciadv.1602902>
20. Lee, M., Chen, C.-Y., Wang, S., Cha, S. N., Park, Y. J., Kim, J. M., Chou, L.-J., & Wang, Z. L. (2012). A hybrid piezoelectric structure for wearable nanogenerators. *Advanced Materials*, 24(13), 1759–1764. <https://doi.org/10.1002/adma.201200150>
21. Liu, H., Zhong, J., Lee, C., Lee, S.-W., & Lin, L. (2018). A comprehensive review on piezoelectric energy harvesting technology: Materials, mechanisms, and applications. *Applied Physics Reviews*, 5(4), Article 041306. <https://doi.org/10.1063/1.5074184>
22. Lopes, A. C., Costa, C. M., Tavares, C. J., Neves, I. C., & Lanceros-Mendez, S. L. (2011). Nucleation of the electroactive  $\gamma$  phase and enhancement of the optical

- transparency in low filler content poly(vinylidene)/clay nanocomposites. *The Journal of Physical Chemistry C*, 115(37), 18076–18082. <https://doi.org/10.1021/jp204513w>
23. Ma, W., Zhang, J., & Wang, X. (2007). Effect of initial polymer concentration on the crystallization of poly (vinylidene fluoride)/poly (methyl methacrylate) blend from solution casting. *Journal of Macromolecular Science, Part B*, 47(1), 139–149. <https://doi.org/10.1080/00222340701746127>
  24. Maity, K., & Mandal, D. (2018). All-organic high-performance piezoelectric nanogenerator with multilayer assembled electro spun nanofiber mats for self-powered multifunctional sensors. *ACS Applied Materials and Interfaces*, 10(21), 18257–18269. <https://doi.org/10.1021/acsami.8b01862>
  25. Mansouri, S., Sheikholeslami, T. F., & Behzadmehr, A. (2019). Investigation on the electrospun PVDF/NP-ZnO nanofibers for application in environmental energy harvesting. *Journal of Materials Research and Technology*, 8(2), 1608–1615. <https://doi.org/10.1016/j.jmrt.2018.07.024>
  26. Mishra, S., Unnikrishnan, L., Nayak, S. K., & Mohanty, S. (2019). Advances in piezoelectric polymer composites for energy harvesting applications: A systematic review. *Macromolecular Materials and Engineering*, 304(1), Article 1800463. <https://doi.org/10.1002/mame.201800463>
  27. Parangusan, H., Ponnamma, D., & Al Maadeed, M. A. A. (2017). Flexible tri-layer piezoelectric nanogenerator based on PVDF-HFP/Ni-doped ZnO nanocomposites. *RSC Advances*, 7, 50156–50165.
  28. Parangusan, H., Ponnamma, D., & Al-Maadeed, M. A. A. (2018). Stretchable electrospun PVDF HFP/Co-ZnO nanofibers as piezoelectric nanogenerators. *Scientific Reports*, 8(1), 754. <https://doi.org/10.1038/s41598-017-19082-3>
  29. Parangusan, H., Ponnamma, D., & AlMaadeed, M. A. A. (2018). Investigation on the effect of  $\gamma$  irradiation on the dielectric and piezoelectric properties of stretchable PVDF/Fe-ZnO nanocomposites for self-powering devices. *Soft Matter*, 14(43), 8803–8813. <https://doi.org/10.1039/c8sm01655k>.
  30. Synthesis
  31. Park, K.-I., Jeong, C. K., Ryu, J., Hwang, G.-T., & Lee, K. J. (2013). Flexible and large-area nanocomposite generators based on lead zirconate titanate particles and carbon nanotubes. *Advanced Energy Materials*, 3(12), 1539–1544. <https://doi.org/10.1002/aenm.201300458>

32. Park, K.-I., Son, J. H., Hwang, G.-T., Jeong, C. K., Ryu, J., Koo, M., Choi, I., Lee, S. H., Byun, M., Wang, Z. L., & Lee, K. J. (2014). Highly-efficient, flexible piezoelectric PZT thin film nanogenerator on plastic substrates. *Advanced Materials*, 26(16), 2514–2520. <https://doi.org/10.1002/adma.201305659>
33. Ponnamma, D., Erturk, A., Parangusan, H., Deshmukh, K., Ahamed, M. B., & Al Maadeed, M. A. A. (2018). Stretchable quaternary phasic PVDF-HFP nanocomposite films containing graphene-titania-SrTiO<sub>3</sub> for mechanical energy harvesting, *Emergent Materials*, 1, 55–65.
34. Prabhakaran, T., & Hemalatha, J. (2013). Ferroelectric and magnetic studies on unpoled poly(vinylidene fluoride)/Fe<sub>3</sub>O<sub>4</sub> magnetoelectric nanocomposite structures. *Materials Chemistry and Physics*, 137, Article 781.e787.
35. Pradeev Raj, K., Sadaiyandi, K., Kennedy, A., Sagadevan, S., Chowdhury, Z. Z., Johan, M. R. B., Aziz, F. A., Rafique, R. F., Thamiz Selvi, R., & Rathina Bala, R. (2018). Influence of Mg doping on ZnO nanoparticles for enhanced photocatalytic evaluation and antibacterial analysis. *Nanoscale Research Letters*, 13(1), 229. <https://doi.org/10.1186/s11671-018-2643-x>
36. Shingange, K., Mhlongo, G. H., Motaung, D. E., & Ntwaeaborwa, O. M. (2016). Tailoring the sensing properties of microwave-assisted grown ZnO nanorods: Effect of irradiation time on luminescence and magnetic behaviour. *Journal of Alloys and Compounds*, 657, 917–926. <https://doi.org/10.1016/j.jallcom.2015.10.069>
37. Soin, N., Shah, T. H., Anand, S. C., Geng, J., Pornwannachai, W., Mandal, P., Reid, D., Sharma, S., Hadimani, R. L., Bayramol, D. V., Siores, E., & Novel. (2014). ‘3-D spacer’ all fibre piezoelectric textiles for energy harvesting applications. *Energy and Environmental Science*, 7, 1670–1679.
38. Sorayani Bafqi, M. S. S., Bagherzadeh, R., & Latifi, M. (2015). Fabrication of composite PVDF-ZnO nanofiber mats by electrospinning for energy scavenging application with enhanced efficiency. *Journal of Polymer Research*, 22(7), 130. <https://doi.org/10.1007/s10965-015-0765-8>
39. Sun, B., Li, X., Zhao, R., Ji, H., Qiu, J., Zhang, N., He, D., & Wang, C. (2019). Electrospun poly (vinylidene fluoride)-zinc oxide hierarchical composite fiber membrane as piezoelectric acoustoelectric nanogenerator. *Journal of Materials Science*, 54(3), 2754–2762. <https://doi.org/10.1007/s10853-018-2985-x>
40. Sun, F.-C., Dongare, A. M., Asandei, A. D., Pamir Alpay, S. P., & Nakhmanson, S. (2015). Temperature dependent structural, elastic, and polar properties of ferroelectric Garima, & Bhukkal, S.

- polyvinylidene fluoride (PVDF) and trifluoroethylene (TrFE) copolymers. *Journal of Materials Chemistry C*, 3(32), 8389–8396. <https://doi.org/10.1039/C5TC01224D>
41. Voiculescu, I., Li, F., Kowach, G., Lee, K.-L., Mistou, N., & Kastberg, R. (2019). Stretchable piezoelectric power generators based on ZnO thin films on elastic substrates. *Micromachines*, 10(10), 661. <https://doi.org/10.3390/mi10100661>
  42. Wang, A., Hu, M., Zhou, L., & Qiang, X. (2019). Self-powered well-aligned P (VDF-TrFE) piezoelectric nanofiber nanogenerator for modulating an exact electrical stimulation and enhancing the proliferation of preosteoclasts. *Nanomaterials*, 9(3), 349. <https://doi.org/10.3390/nano9030349>
  43. Wang, P., & Du, H. (2015). ZnO thin film piezoelectric MEMS vibration energy harvesters with two piezoelectric elements for higher output performance. *The Review of Scientific Instruments*, 86(7), Article 075002. <https://doi.org/10.1063/1.4923456>
  44. Wang, S., Wang, Z. L., & Yang, Y. A. (2016). A one-structure-based hybridized nanogenerator for scavenging mechanical and thermal energies by triboelectric–piezoelectric–pyroelectric effects. *Advanced Materials*, 28(15), 2881–2887. <https://doi.org/10.1002/adma.201505684>
  45. Wang, Y. R., Zheng, J. M., Ren, G. Y., Zhang, P. H., & Xu, C. (2011). A flexible piezoelectric force sensor based on PVDF fabrics. *Smart Materials and Structures*, 20(4), Article 045009. <https://doi.org/10.1088/0964-1726/20/4/045009>
  46. Wang, Z. L., & Song, J. (2006). Piezoelectric nanogenerators based on zinc oxide nanowire arrays. *Science*, 312(5771), 242–246. <https://doi.org/10.1126/science.1124005>
  47. Ye, S., Cheng, C., Chen, X., Chen, X., Shao, J., Zhang, J., Hu, H., Tian, H., Li, X., Ma, L., & Jia, W. (2019). High-performance piezoelectric nanogenerator based on microstructured P (VDF TrFE)/BNNTs composite for energy harvesting and radiation protection in space. *Nano Energy*, 60, 701–714. <https://doi.org/10.1016/j.nanoen.2019.03.096>
  48. You, M.-H., Wang, X.-X., Yan, X., Zhang, J., Song, W.-Z., Yu, M., Fan, Z.-Y., Ramakrishna, S., & Long, Y.-Z. (2018). A self-powered flexible hybrid piezoelectric–pyroelectric nanogenerator based on non-woven nanofiber membranes. *Journal of Materials Chemistry A*, 6(8), 3500–3509. <https://doi.org/10.1039/C7TA10175A>